Fig. S1

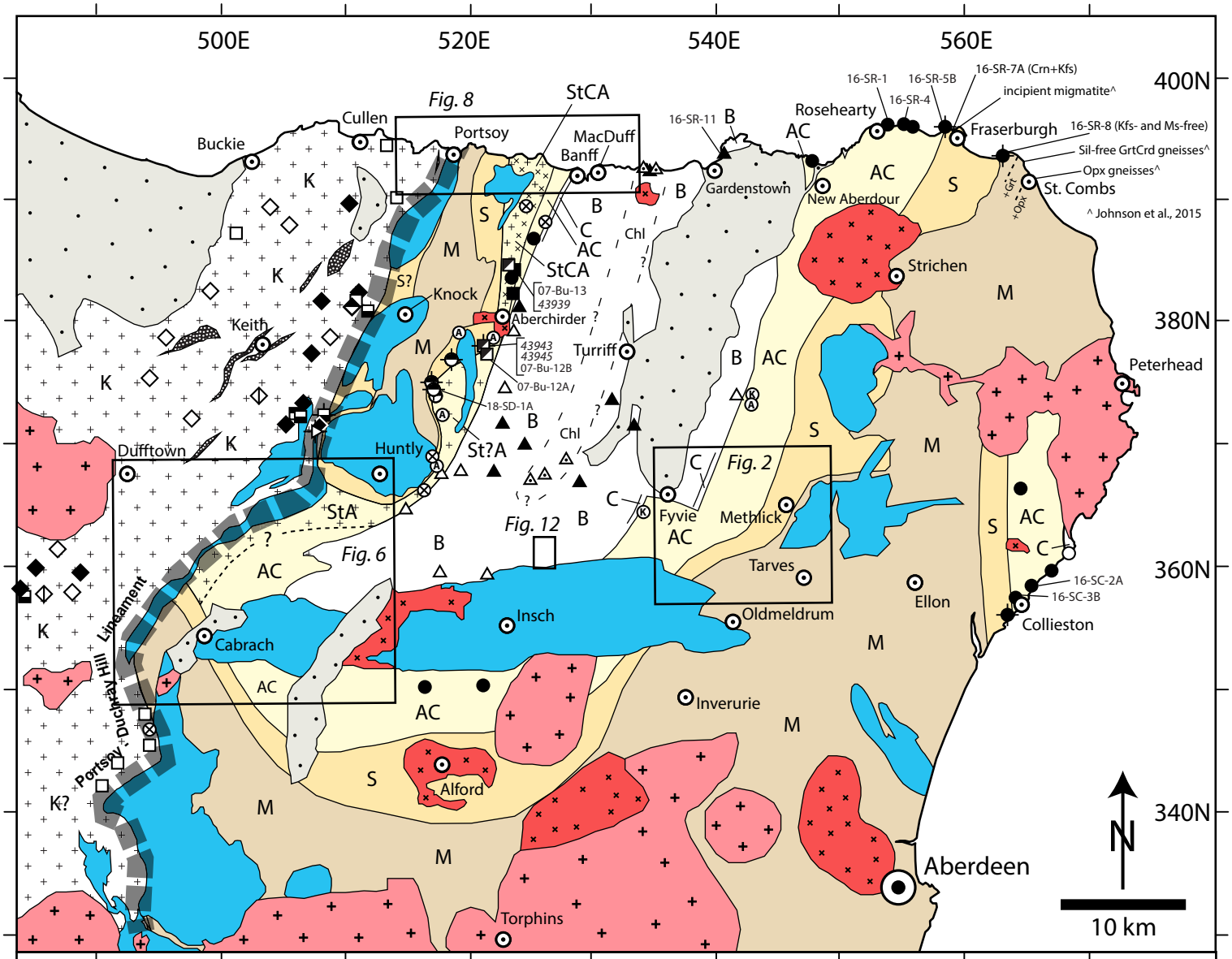

Metamorphic zones in Buchan domain

Chl Chlorite
B Biotite
C Cordierite
AC Andalusite-cordierite
StA Staurolite-andalusite
StCA Staurolite-cordierite-andalusite
S Sillimanite
M Gneiss/migmatite
+Grt Grt-in isograd in NE
+Opx Opx-in isograd in NE

Barrovian domain: K Kyanite-staurolite domain

Non-metamorphic rock types

Devonian strata
Younger Granites
Granites
Mafic/ultramafic intrusions
Older Granites

Mineral assemblages in Barrovian domain (all + Ms Pl Qtz)

Ky St Bt
Ky St Bt Grt
Ky St Bt Grt (And Sil)
Ky St Bt Grt (And)
Ky Bt (And)
Ky*
St Bt
St Bt Grt
St*
Grt St Sil Bt
Grt Sil Bt

Mineral assemblages in Buchan domain (all + Ms Pl Qtz)

Slate/phyllite**
knotted slate/phyllite**
nodular And-bearing schist**
Chl
Chl Bt
Crd Bt
Crd And Bt
And*
And Bt ±Grt
St And Bt ±Grt
St Crd And Bt ±Grt
And+Sil*
Crd And Sil Bt
And Sil Bt ±Grt
Sil St And Bt ±Grt
Sil St Crd And Bt ±Grt

* index mineral occurrences from the literature (full mineral assemblages not reported)
** field-based rock descriptions from Read (1923), Fettes et al. (1991) and Gunn et al. (2015)

16-SR-4 sample numbers from this study
43939 sample numbers in italics from Hudson (1975; 1980)

Figure S1. Metamorphic map of the Buchan block and adjacent Barrovian domain from Fig. 1b, with mineral assemblages from outside the four inset maps plotted. The domain labelled "St?A" indicates an area of andalusite schists that resemble in appearance staurolite+andalusite-bearing schists to the NE and SW but in which staurolite has not been observed (see text). The data sources for the mineral assemblages and metamorphic zones/isograds used to build the map are as follows: Ashworth (1975; 1976); Ashworth & Chinner (1978); Beddoe-Stephens (1990); Carty & Johnson (2015); Chinner (1980); Chinner & Heseltine (1979); Droop et al. (2003); Fettes (1970; 1971; 2013); Fettes et al. (1991); Fettes (unpubl. data); Gillen (1987); Gunn et al. (2015); Harte & Hudson (1979); Hudson (1975; 1980; 1987); Hudson & Harte (1985); Hudson & Johnson (2015); Johnson & Fischer (2015); Johnson & Kneller (2015); Johnson et al. (2001a; 2001b; 2003; 2015); Kneller (1987a; 1987b); Leslie (1984; 1987a; 1987b; 1988); Mendum (1987; 2013a; 2013b); Munro (1986); Porteous (1973); Read (1923; 1952; 1955; 1960); Read & Farquhar (1956); Stephenson (2013); Stephenson et al. (2013); Treagus (2009); Treagus & Roberts (1981); Viete et al. (2010); British Geological Survey 1:50,000 Sheets 75E, 76W, 85E, 86E, 86W, 87W, 96W, 97.

References for Fig. S1 that are not listed in the References for the main paper

British Geological Survey (1991). *Ellon, Scotland. Sheet 87W. Solid geology. 1:50,000.* British Geological Survey.

British Geological Survey (1996). *Glenfiddich, Scotland. Sheet 85E. Solid geology. 1:50,000.* British Geological Survey.

British Geological Survey (2002). *Portsoy, Scotland. Sheet 96W. Solid and Drift Geology. 1:50,000.* British Geological Survey.

Fig. S2

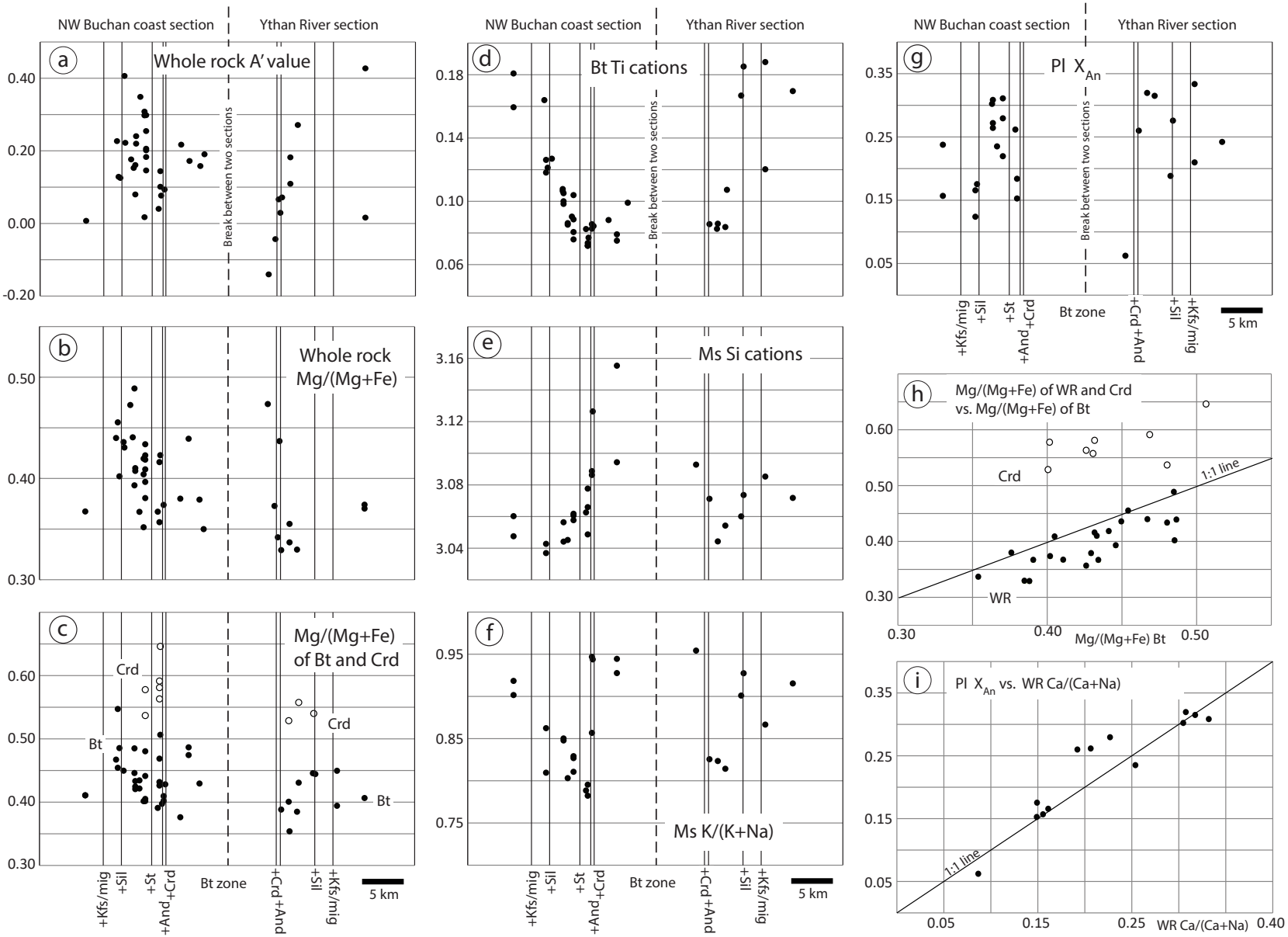

Fig. S2. Plots of whole rock and mineral chemical parameters as a function of distance/grade across the Buchan block. The graphs portray data from the two most intensively-sampled transects: the Ythan River transect (Fyvie-Methlick-Tarves area) of the central SE Buchan sequence (Figs. 1b and 2); and the NW Buchan coastal sequence (Figs. 1b and Fig. 8). The two transects increase in grade outwards in opposite directions (east and west) from the central low-grade Bt±Chl domain (see Fig. 1b). Raw data in Supplementary Tables S2 to S11.

Fig. S3a and S3b

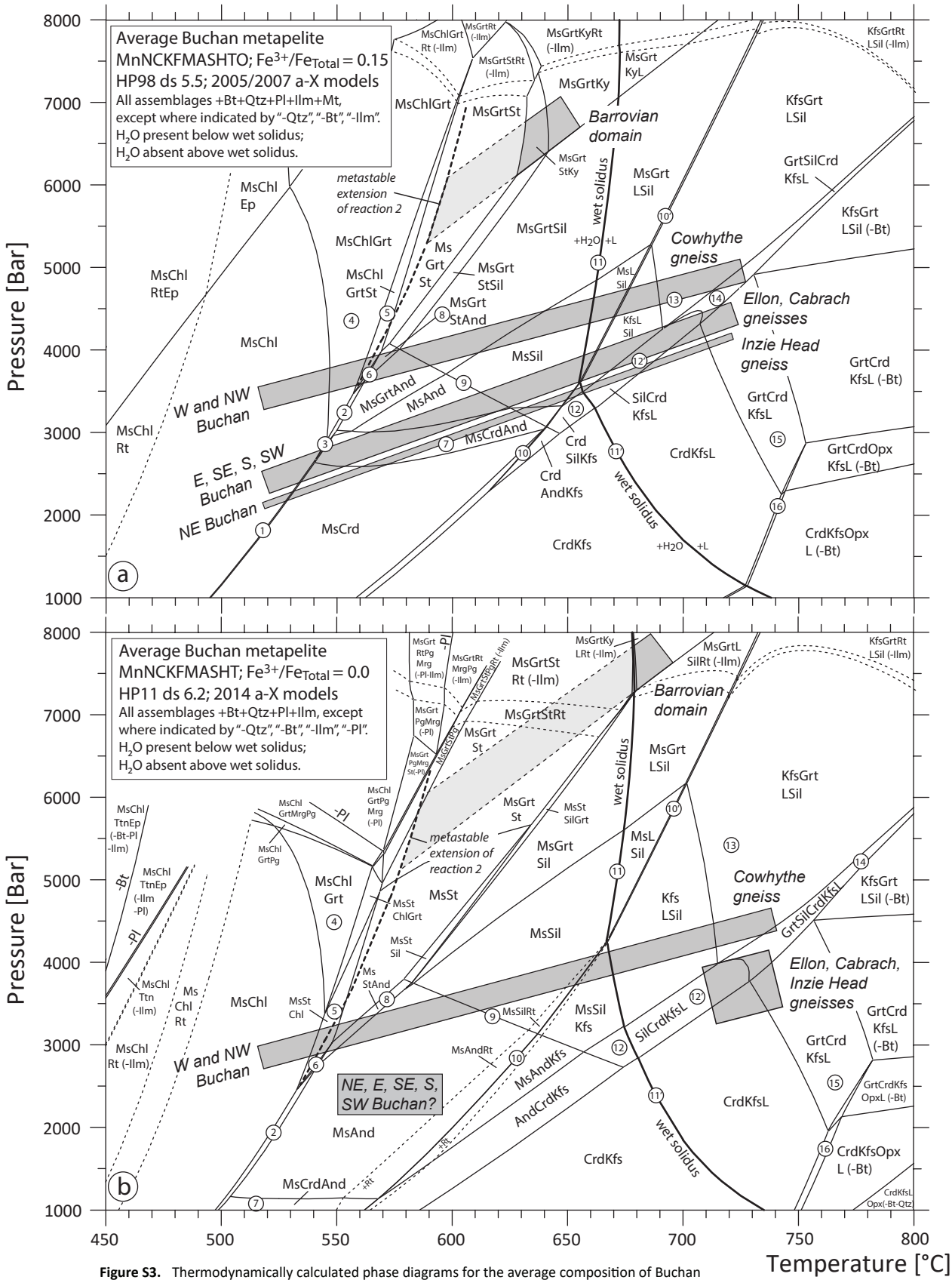

Figure S3. Thermodynamically calculated phase diagrams for the average composition of Buchan pelites of this study, except for (d) which is for an average metagreywacke composition. The compositions are listed in Table S4. The method of calculation of the phase diagrams is provided in Supplementary Document S2. Numbered reactions are listed in the text. Mineral abbreviations from Kretz (1983). Metamorphic field gradients are drawn on the diagrams to satisfy the order of inferred reactions in the text. See text for explanation of the pale-coloured P-T box for the Barrovian domain. **(a)** Phase diagram calculated using thermodynamic dataset and a-X models "HP5.5", using the measured whole rock value of X_{Fe3+} = 0.15 (see text for explanation and discussion). The complementary phase diagram calculated assuming all Fe as Fe^{2+} is provided in Fig 16a.**(b)** Phase diagram calculated using thermodynamic dataset and a-X models "HP6.2", assuming all Fe as Fe^{2+} (see text for explanation and discussion). The complementary phase diagram calculated for the measured whole rock value of X_{Fe3+} = 0.15 is provided in Fig. 16b.

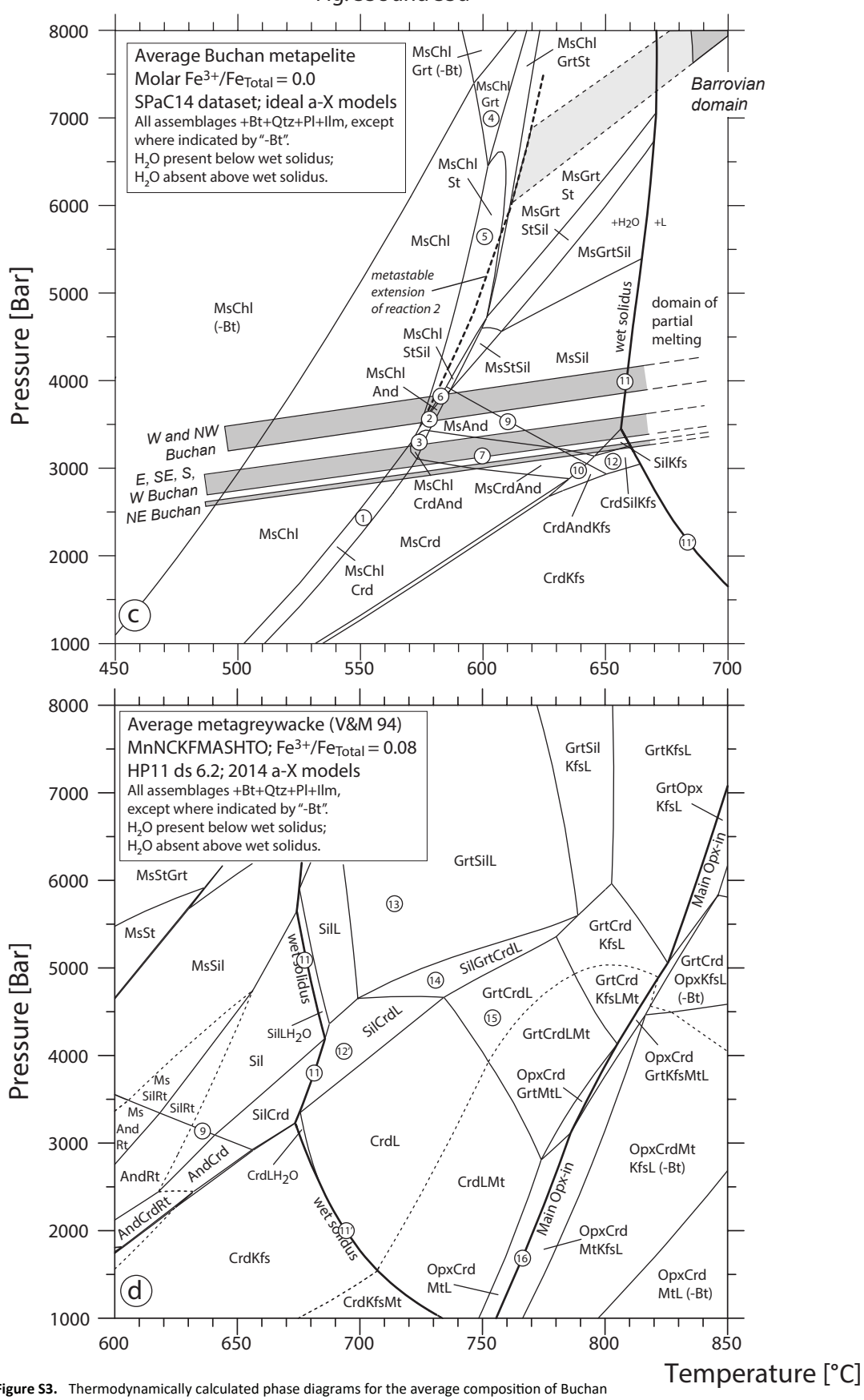

Figure S3. Thermodynamically calculated phase diagrams for the average composition of Buchan pelites of this study, except for (d) which is for an average metagreywacke composition. The compositions are listed in Table S4. The method of calculation of the phase diagrams is provided in Supplementary Document S2. Numbered reactions are listed in the text. Mineral abbreviations from Kretz (1983). Metamorphic field gradients are drawn on the diagrams to satisfy the order of inferred reactions in the text. See text for explanation of the pale-coloured P-T box for the Barrovian domain. **(c)** Subsolidus phase diagram calculated using thermodynamic dataset and a-X models "SPaC14", assuming all Fe as Fe^{2+} (see text for explanation and discussion). **(d)** Phase diagram for the average metagreywacke composition of Vielzeuf & Montel (1994), calculated using thermodynamic dataset and a-X models "HP6.2" and the measured whole rock value of X_{Fe3+} = 0.08.

Fig. S4a to f. Representative back-scattered electron images of textural setting of monazite in rocks from the Buchan domain

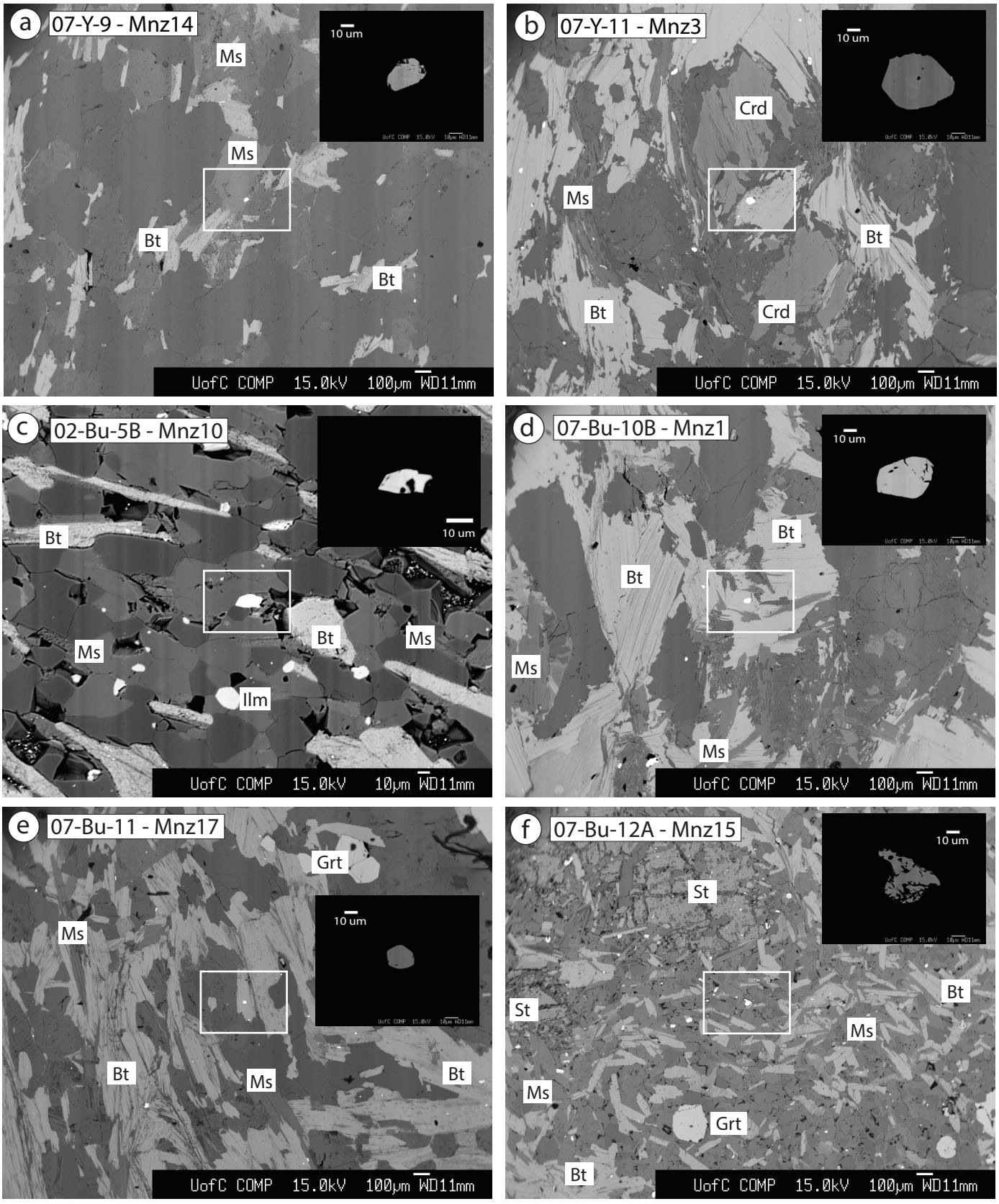

Figure S4. Back-scattered electron (BSE) images of the textural setting of monazite grains from the nine samples chosen for monazite U-Pb geochronology (isotopic results and interpreted ages provided in Table S13). "Mnz14" etc. refers to the grain number in Table S13. In addition to the minerals labelled, all rocks contain quartz and plagioclase (darker grey colours in the BSE images). Mineral abbreviations from Kretz (1983). Images S4a to f are for the six samples from the Buchan domain; images S4g to k are for the three coastal samples from the Barrovian domain west of Portsoy.

Fig. S4g to k. Representative back-scattered electron images of textural setting of monazite in Barrovian rocks of the northwest Buchan coastal section

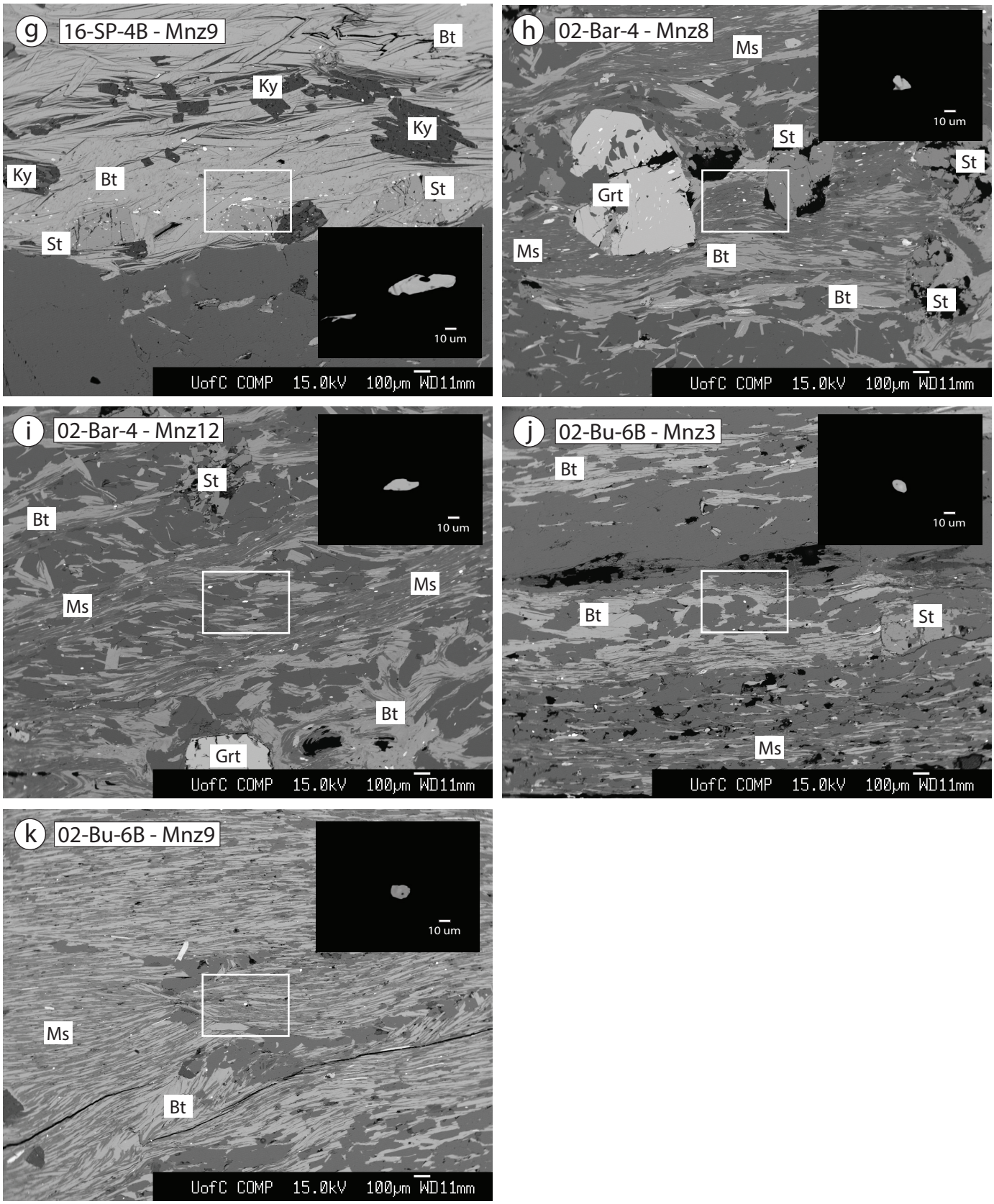

Figure S4. Back-scattered electron (BSE) images of the textural setting of monazite grains from the nine samples chosen for monazite U-Pb geochronology (isotopic results and interpreted ages provided in Table S13). "Mnz14" etc. refers to the grain number in Table S13. In addition to the minerals labelled, all rocks contain quartz and plagioclase (darker grey colours in the BSE images). Mineral abbreviations from Kretz (1983). Images S4a to f are for the six samples from the Buchan domain; images S4g to k are for the three coastal samples from the Barrovian domain west of Portsoy.

Fig. S5a to f. Monazite U-Pb results for samples from the Buchan domain plotted on Tera-Wasserberg concordia diagrams

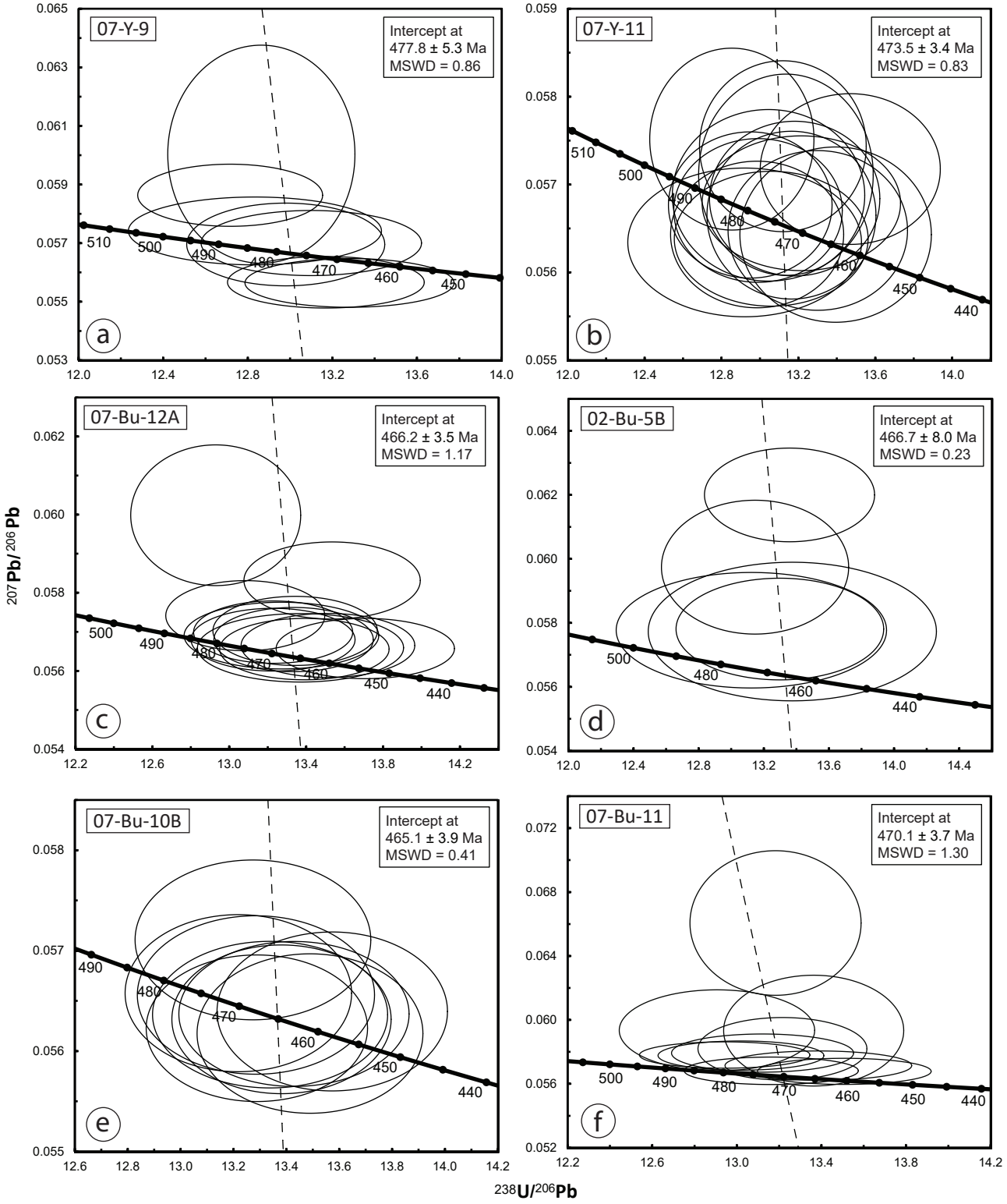

Figure S5. Results of monazite U-Pb geochronology plotted on Tera–Wasserburg U–Pb concordia diagrams (Tera & Wasserberg, 1972; Ludwig, 2003). Raw data for these plots are presented in Table S13, and analytical methods are provided in Supplementary Document S1. The samples are located in Figs. 1b, 2 and 4. Concordia intercept ages are anchored to an assumed common Pb value of 0.835 ± 0.06. Uncertainty ellipses are 2-sigma. MSWD – Mean Square of Weighted Deviates. Figures S5a to f are for the six samples analysed from the Buchan domain.

Fig. S5g to l. Monazite U-Pb results for combined samples from the Buchan domain, and for coastal samples from the Barrovian domain west of Portsoy, plotted on Tera-Wasserberg concordia diagrams

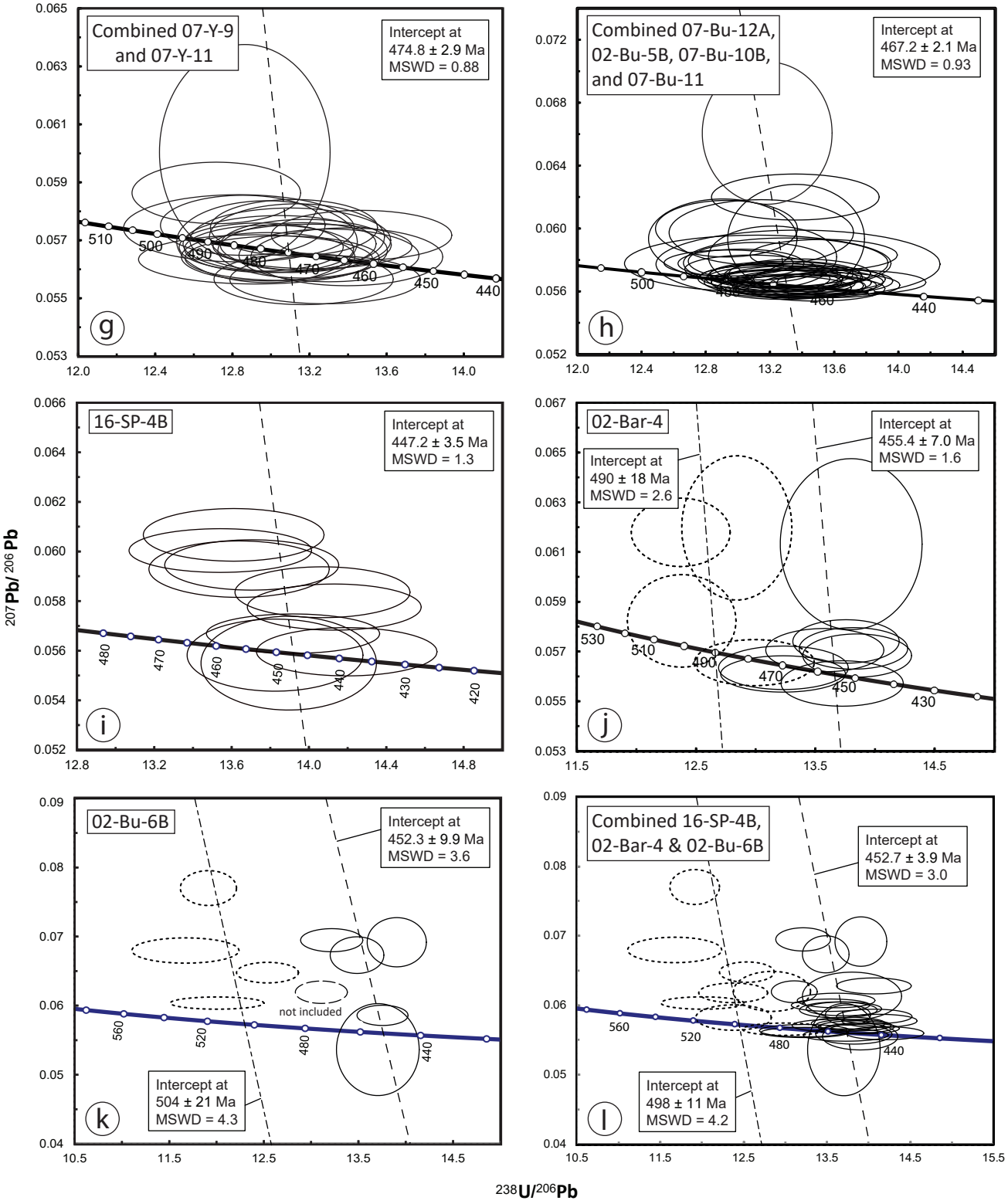

Figure S5. Results of monazite U-Pb geochronology plotted on Tera–Wasserburg U–Pb concordia diagrams (Tera & Wasserberg, 1972; Ludwig, 2003). Raw data for these plots are presented in Table S13, and analytical methods are provided in Supplementary Document S1. The samples are located in Figs. 1b, 2 and 4. Concordia intercept ages are anchored to an assumed common Pb value of 0.835 ± 0.06. Uncertainty ellipses are 2-sigma. MSWD – Mean Square of Weighted Deviates. Figure S5g combines the results for the two samples of the Ellon gneiss from the SE Buchan domain (07-Y-9 and 07-Y-11); Figure S5h combines the results from the four samples from the northwest Buchan coastal sequence (02-Bu-5B, 07-Bu-10B, 07-Bu-11 and 07-Bu-12A); Figures S5i to k are for the three samples analysed from the Barrovian domain west of Portsoy; and Figure S5l combines the results from the three samples from the Barrovian domain west of Portsoy.